

cell (Osmonics) with an effective filtration area of 16.9 cm<sup>2</sup> or ii) on 43 mm diameter membranes using an Amicon 8050 stirred, dead-end filtration cell (Millipore) having an effective filtration area of 13.4 cm<sup>2</sup>. Each filtration cell was stirred at 500 rpm using a speed-adjustable stir plate (VWR) to prevent concentration polarization at the sample surface. Trans-membrane pressure gradients were provided with nitrogen gas during the filtration experiments. Filtration experiments were conducted at 66 psi.

**Characterization of Gold Nanoparticles:** Nanoparticle diameters in the feed and permeate solutions were determined by transmission electron microscopy (TEM) using a JEOL 100CX microscope operating in bright field mode at 200 kV. TEM specimens for each sample were prepared by evaporating the nanoparticle solution at room temperature onto a 400-mesh copper TEM grid (Ted Pella, Inc.). Image analysis and particle counting were performed using NIH Scion Image software. In the TEM images, apparent agglomerated particles with dimensions over an order of magnitude larger than the average size were neglected. The size distribution of the gold nanoparticles was investigated by UV-vis spectroscopy using a Cary 5E spectrophotometer (Varian).

Received: April 27, 2004  
Final version: August 3, 2004

- [1] A. C. Templeton, M. P. Wuelffing, R. W. Murray, *Acc. Chem. Res.* **2000**, 33, 27.
- [2] M.-C. Daniel, D. Astruc, *Chem. Rev.* **2004**, 104, 293.
- [3] A. P. Alivisatos, P. F. Barbara, A. W. Castleman, J. Chang, D. A. Dixon, M. L. Klein, G. L. McLendon, J. S. Miller, M. A. Ratner, P. J. Rossky, S. I. Stupp, M. E. Thompson, *Adv. Mater.* **1998**, 10, 1297.
- [4] S. A. Empedocles, M. G. Bawendi, *Science* **1997**, 278, 2114.
- [5] A. P. Alivisatos, *Science* **1996**, 271, 933.
- [6] S. A. Empedocles, R. Neuhauser, K. Shimizu, M. G. Bawendi, *Adv. Mater.* **1999**, 11, 1243.
- [7] R. P. Andres, T. Bein, M. Dorogi, S. Feng, J. I. Henderson, C. P. Ku-biak, W. Mahoney, R. G. Osifchin, R. Reifenberger, *Science* **1996**, 272, 1323.
- [8] A. N. Shipway, E. Katz, I. Willner, *ChemPhysChem* **2000**, 1, 18.
- [9] A. N. Shipway, M. Lahav, I. Willner, *Adv. Mater.* **2000**, 12, 993.
- [10] M. Bruchez, M. Moronne, P. Gin, S. Weiss, A. P. Alivisatos, *Science* **1998**, 281, 2013.
- [11] M. A. Hines, G. D. Scholes, *Adv. Mater.* **2003**, 15, 1844.
- [12] M. G. Bawendi, M. L. Steigerwald, L. E. Brus, *Annu. Rev. Phys. Chem.* **1990**, 41, 477.
- [13] S. W. Chen, R. S. Ingram, M. J. Hostetler, J. J. Pietron, R. W. Murray, T. G. Schaaff, J. T. Khoury, M. M. Alvarez, R. L. Whetten, *Science* **1998**, 280, 2098.
- [14] S. W. Chen, R. W. Murray, S. W. Feldberg, *J. Phys. Chem. B* **1998**, 102, 9898.
- [15] B. K. H. Yen, N. E. Stott, K. F. Jensen, M. G. Bawendi, *Adv. Mater.* **2003**, 15, 1858.
- [16] H. Zhang, Z. C. Cui, Y. Wang, K. Zhang, X. L. Ji, C. L. Lu, B. Yang, M. Y. Gao, *Adv. Mater.* **2003**, 15, 777.
- [17] M. J. Hostetler, A. C. Templeton, R. W. Murray, *Langmuir* **1999**, 15, 3782.
- [18] H. P. Zheng, I. Lee, M. F. Rubner, P. T. Hammond, *Adv. Mater.* **2002**, 14, 569.
- [19] V. L. Jimenez, M. C. Leopold, C. Mazzitelli, J. W. Jorgenson, R. W. Murray, *Anal. Chem.* **2003**, 75, 199.
- [20] J. P. Wilcoxon, J. E. Martin, P. Provencio, *Langmuir* **2000**, 16, 9912.
- [21] T. G. Schaaff, M. N. Shafigullin, J. T. Khoury, I. Vezmar, R. L. Whetten, W. G. Cullen, P. N. First, C. Gutierrez-Wing, J. Ascensio, M. J. Jose-Yacamán, *J. Phys. Chem. B* **1997**, 101, 7885.
- [22] T. G. Schaaff, G. Knight, M. N. Shafigullin, R. F. Borkman, R. L. Whetten, *J. Phys. Chem. B* **1998**, 102, 10643.
- [23] M. E. Davis, *Nature* **2002**, 417, 813.
- [24] W. H. Baur, *Nat. Mater.* **2003**, 2, 17.
- [25] P. K. Kang, D. O. Shah, *Langmuir* **1997**, 13, 1820.
- [26] A. Akthakul, W. F. McDonald, A. M. Mayes, *J. Membr. Sci.* **2002**, 208, 147.
- [27] J. F. Hester, P. Banerjee, Y. Y. Won, A. Akthakul, M. H. Acar, A. M. Mayes, *Macromolecules* **2002**, 35, 7652.
- [28] S. Inceoglu, S. C. Olugebefola, M. H. Acar, A. M. Mayes, *Des. Monomers Polym.* **2004**, 7, 181.
- [29] A. Akthakul, R. F. Salinaro, A. M. Mayes, *Macromolecules* **2004**, 37, 7663.
- [30] M. Brust, M. Walker, D. Bethell, D. J. Schiffrin, R. Whyman, *J. Chem. Soc., Chem. Commun.* **1994**, 801.
- [31] U. Kreibitz, M. Vollmer, *Optical Properties of Metal Clusters*, Springer-Verlag, New York **1995**, p. 25.
- [32] S. Link, M. A. El-Sayed, *Int. Rev. Phys. Chem.* **2000**, 19, 409.
- [33] R. S. Ingram, M. J. Hostetler, R. W. Murray, *J. Am. Chem. Soc.* **1997**, 119, 9175.
- [34] W. P. Wuelffing, F. P. Zamborini, A. C. Templeton, X. G. Wen, H. Yoon, R. W. Murray, *Chem. Mater.* **2001**, 13, 87.
- [35] A. M. Jackson, J. W. Myerson, F. Stellacci, *Nat. Mater.* **2004**, 3, 330.
- [36] J. F. Marko, *Macromolecules* **1993**, 26, 313.
- [37] S. K. Satija, P. D. Gallagher, A. Karim, L. J. Fetters, *Physica B+C (Amsterdam)* **1998**, 248, 204.
- [38] J. P. Wilcoxon, J. E. Martin, P. Provencio, *J. Chem. Phys.* **2001**, 115, 998.
- [39] J. P. Wilcoxon, P. Provencio, *J. Phys. Chem. B* **1999**, 103, 9809.

## Mechanically Strong Hydrogels with Ultra-Low Frictional Coefficients

By Daisaku Kaneko, Tomohiro Tada,  
Takayuki Kurokawa, Jian P. Gong,\* and  
Yoshihito Osada

Industrial or environmental problems caused by materials with high-friction surfaces have always existed. Searching for materials with low-friction surfaces has been a classic and everlasting research topic for materials scientists and engineers. Despite many efforts, it has been shown that surface modification or addition of lubricants is not very effective in reducing the steady-state sliding friction between two solids, which can exhibit a frictional coefficient,  $\mu$ , of  $\sim 10^{-1}$ , even in the presence of a lubricant.<sup>[1]</sup> One of the most brilliant inventions used to obtain low friction is the bearing system, which exhibits a frictional coefficient much lower than that of sliding friction. The bearing system achieves low friction by using a layer of oil between a surface and a rolling sphere. However,

\* Prof. J. P. Gong, D. Kaneko, T. Tada, T. Kurokawa, Prof. Y. Osada  
Division of Biological Sciences  
Graduate School of Science  
Hokkaido University  
Sapporo 060-0810 (Japan)  
E-mail: gong@sci.hokudai.ac.jp  
Prof. J. P. Gong  
SORST, JST  
Sapporo 060-0810 (Japan)

the complicated structure of the bearing system serves as a limitation to its use in many applications where a simple geometry is preferred, such as in micromachine systems and in biomedical applications.

Our previous study showed that the presence of polyelectrolyte brushes on a hydrogel surface can effectively reduce the sliding-friction coefficient of the surface to a value as low as  $10^{-4}$ .<sup>[2]</sup> This discovery should have enabled the hydrogel to find wide applications in many fields where low friction is required. Unfortunately, conventional hydrogels are mechanically too weak to be practically used in any stress- or strain-bearing applications, which hinders extensive application of hydrogels as industrial and biomedical materials. Recently, we discovered a general method to obtain very strong hydrogels containing 60–90 % water by inducing a double-network (DN) structure for various combinations of hydrophilic polymers. The DN hydrogel exhibited fracture strengths as high as a few to several tens of megapascals, i.e., up to  $\sim 100 \text{ kgfcm}^{-2}$ .<sup>[3]</sup> Based on this research, we report on two novel materials, formed by adding a third component—either a weakly crosslinked network (to form a triple-network, or TN, gel) or non-crosslinked linear polymer chains (to form a DN-L gel)—to a high-strength DN gel. The new materials show fracture strengths as high as 9 MPa and frictional coefficients as low as  $10^{-5}$ . The soft- and wet-gel materials, with both high strength and extremely low surface friction, could find wide applications not only in industry, but also in the biomedical field, for example, as substitutes for articular cartilage or other bio-tissues.

The DN gel, which had a high fracture strength, consisted of two interpenetrated and independently crosslinked networks, in which negatively charged poly(2-acrylamido-2-methylpropane sulfonic acid) (PAMPS) and neutral poly(acrylamide) (PAAm) networks acted as the first and second networks, respectively. In order to impart a low surface sliding friction to the gels, the TN gel and DN-L gels were synthesized by introducing PAMPS as a third component into the DN gel, in the presence and absence of crosslinker, respectively. All three kinds of gels, DN, TN, and DN-L, were highly transparent and showed no apparent difference in appearance (Fig. 1). The mechanical properties of the gels are summarized in Table 1. All the gels showed fracture strengths on the order of megapascals (MPa), despite containing more than 80 % water. An increase in the elasticities of the TN and DN-L gels over that of the DN gel is a result of the presence

**Table 1.** Mechanical properties of DN, TN, and DN-L gels.

Gels	Water content [wt.-%]	Elasticity [MPa]	Fracture stress $\sigma_{\text{max}}$ [MPa]	Fracture strain $\lambda_{\text{max}}$ [%]
DN	84.8	0.84	4.6	65
TN	82.5	2.0	4.8	57
DN-L	84.8	2.1	9.2	70

of the third component, PAMPS, and not of its crosslinking, since their elasticities are almost the same ( $\sim 2 \text{ MPa}$ ). The DN-L gel was superior to the DN gel in terms of fracture strength, although both gels contained almost the same amount of water. This remarkable increase in the fracture strength of DN-L over that of the other two gels resulted from the presence of linear chains of PAMPS, which can effectively dissipate fracture energy.<sup>[3,4]</sup>

Plots of the frictional forces of the gels per unit contact area,  $f$ , versus a wide range of normal pressure,  $P$ , are shown in Figure 2a. The frictional coefficients,  $\mu$ , calculated from the results of Figure 2a, are plotted against  $P$  in Figure 2b. Comparison of  $\mu$  for DN and TN indicates that the introduction of PAMPS as the third network component reduced the frictional coefficient of the TN gel. Our previous study, which showed that surface friction between negatively charged gels and negatively charged glass substrates in pure water exhibits very low frictional coefficients due to osmotic repulsion<sup>[5]</sup> could explain these results. The DN gel has relatively large values of frictional coefficient ( $\sim 10^{-1}$ ) since the gel's second component, PAAm, is adsorptive on the glass substrate. The TN gel was extended in such a way that the third component added to the DN gel (the crosslinked PAMPS network) enhances repulsive interaction with the glass substrate. The enhanced negative charge density reduced the frictional coefficient of the TN gel to a value of  $\sim 10^{-3}$ , much lower than that of the DN gel. These results indicate that osmotic repulsive interaction between the two surfaces was effective even under a pressure as high as  $\sim 10^5 \text{ Pa}$ .

The DN-L gel is based on high-strength DN gels containing linear PAMPS chains. Since we reported that the linear PAMPS polymer chains on the gel surface can reduce frictional forces due to further repulsive interaction with the glass substrate,<sup>[2]</sup> we have been mostly interested in whether these linear polyelectrolyte chains are still effective in showing low surface friction under a pressure as high as that in a human joint ( $\sim \text{MPa}$ ). Figure 2 shows that the presence of free, linear PAMPS polymer chains (not crosslinked, as for TN) significantly reduced the frictional coefficient to a value ( $\sim 10^{-4}$ ) as small as one to three orders of magnitude less than that of the TN and DN gels, respectively, under a pressure range of  $10^3$ – $10^5 \text{ Pa}$ , which is close to the pressure exerted on articular cartilage in synovial joints.

The dependence of  $\mu$  on sliding velocity has been investigated over a wide range of veloci-

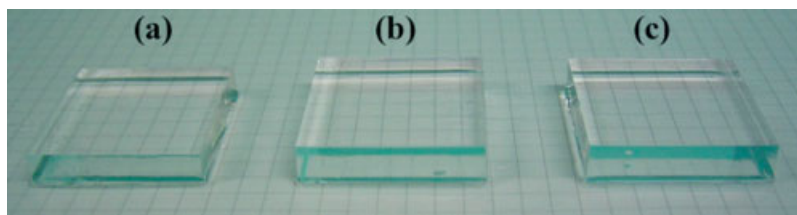


**Figure 1.** Pictures of the a) DN gel, b) TN gel, and c) TN-L gel. The size of the lattice is 3 mm  $\times$  3 mm.

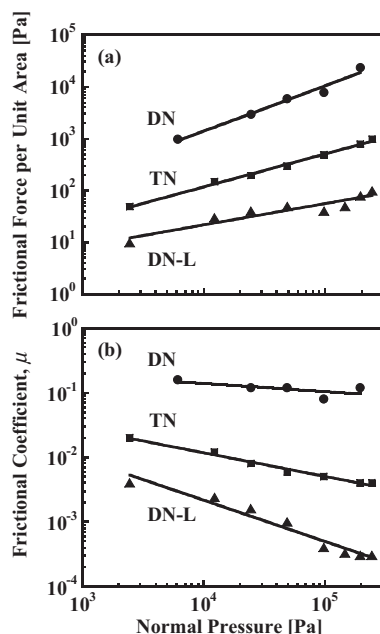


**Figure 2.** Normal-pressure dependence of a) frictional force per unit area and b) frictional coefficient of the hydrogels against a glass plate in pure water. Sliding velocity:  $1.7 \times 10^{-3} \text{ m s}^{-1}$ . Symbols denote DN (●), TN (■), and DN-L (▲) gels, respectively. Solid lines are to guide the eyes.

ties, and the results are shown in Figure 3. The DN, TN, and DN-L gels were strong enough to endure high sliding shear stresses. For DN, the frictional force per unit area versus sliding velocity curve shows a broad peak, which is characteristic of the adsorptive interaction between the gel (the PAAm component) and the substrate.<sup>[5]</sup> The frictional coefficient of DN-L is significantly lower ( $10^{-5}$ – $10^{-4}$ ) than those of the DN ( $10^{-2}$ – $10^{-1}$ ) and TN ( $10^{-4}$ – $10^{-3}$ ) gels at a low sliding velocity of  $5 \times 10^{-4} \text{ m s}^{-1}$ , even under extremely high pressure ( $\sim 10^5 \text{ Pa}$ ). However,  $\mu$  for DN-L shows a strong dependence on velocity, and its value comes close to that of TN with increasing sliding velocity. This is because the linear polymer chains of DN-L are highly mobile under low sliding velocities (less than

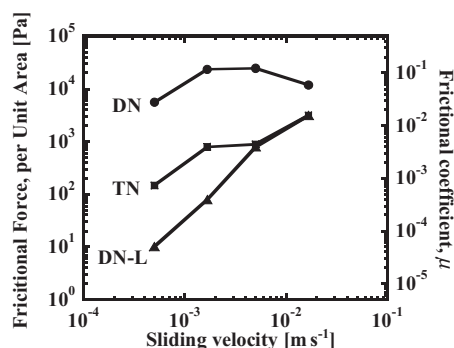


**Figure 3.** Sliding-velocity dependence of the frictional force per unit area and frictional coefficients of the hydrogels against glass in pure water. Normal pressure is  $2.0 \times 10^5 \text{ Pa}$ . Symbols denote DN (●), TN (■), and DN-L (▲) gels. Solid lines are to guide the eyes.

$5.0 \times 10^{-3} \text{ m s}^{-1}$ ), which contributes to the reduction of friction. However, when the sliding velocity increased to a value such that the conformational change of the linear polymer failed to follow the sliding velocity (or shear rate), the linear polymer chains behaved like a cross-linked network.

From these results, it might be thought intuitively that DN-L is not suitable for use in high-velocity applications; however, the frictional coefficient in the high-velocity range of  $5.0 \times 10^{-3}$ – $2.0 \times 10^{-2} \text{ m s}^{-1}$  is  $10^{-3}$ – $10^{-2}$ , which is still 1–2 orders of magnitude smaller than that of a solid. Furthermore, the value of  $\mu$  ( $10^{-3}$ – $10^{-2}$ ) is comparable with that of articular cartilage, which has a value of  $\sim 10^{-1}$  at a steady-state sliding velocity of  $10^{-2} \text{ m s}^{-1}$ .<sup>[6–8]</sup> These results demonstrate that all the gels were strong enough to endure extremely high pressures, and the surface properties of the gels were dominated by the last component added, i.e., the second component (PAAm) in the case of the DN gel, and the third component (PAMPS) in the case of the TN and DN-L gels.

We have reported a novel functional hydrogel (DN-L) that has a high fracture strength (9.2 MPa) and an ultra-low-friction surface ( $\mu \sim 10^{-5}$ ) under an extremely high pressure of the order of sub-MPa. This value of  $\mu$  is of industrial and biomedical relevance, and is as observed in human articular cartilage. We have also clarified a significant fact, i.e., that linear polymer chains on gel surfaces can play a role in friction reduction even under extremely high normal pressure. These results will open a new era for hydrogels to be used as low-friction materials in industry as well as in the biomedical field.

## Experimental

**2-Acrylamido-2-methylpropane sulfonic acid (AMPS)** (monomer; Tokyo Kasei Co., Ltd.) and **2-oxoglutaric acid** (initiator) were used as received. **Acrylamide (AAM)** (monomer) was recrystallized from chloroform. ***N,N'*-Methylene bisacrylamide (MBAA)** (crosslinking agent) was recrystallized from ethanol.

**Synthesis of the DN Gel:** Chemically crosslinked poly(2-acrylamido-2-methylpropane sulfonic acid) (PAMPS) gel (first-network gel) was synthesized by UV irradiation (wavelength = 365 nm) from an aqueous solution of 1 M AMPS monomer containing 8 mol-% MBAA and 0.1 mol-% 2-oxoglutaric acid, in a reaction cell made of a pair of glass plates with a 2 mm spacing. The first network gel was then immersed in a second aqueous solution of 2 M AAM, containing 0.1 mol-% MBAA and 0.1 mol-% 2-oxoglutaric acid, for 1 day, until equilibrium was reached. The second network was synthesized by UV irradiation of the AAM-containing first-network gel.

**Synthesis of the TN and DN-L Gels:** The TN and DN-L gels were synthesized by UV irradiation after immersing the DN gels in a large amount of a third solution of 1 M AMPS and 0.1 mol-% 2-oxoglutaric acid, with (TN) and without (DN-L) the presence of 0.1 mol-% MBAA. After polymerization, the samples were immersed in a large amount of distilled water for 1 week to equilibrate and to remove residual chemicals.

**Characterization:** The mechanical strength of the gels was characterized by compressive stress–strain measurements, which were performed on water-swollen gels using a tensile-compressive tester (Tension RTC-1310A, Orientec Co.). The cylindrical gel sample, 9 mm in diameter and 3 mm thick, was set on the lower plate and compressed by the upper plate, which was connected to a load cell, at a strain rate of  $10\% \text{ min}^{-1}$ . Strain was defined as the thickness change divided by the thickness of the free-standing state. Details are described elsewhere [9].

Friction measurements were performed using gel samples equilibrated in distilled water against a glass substrate at room temperature, using a tribometer (Heidon 14S/14DR, Shindom Sci., Co.). The size of the gels was 20 mm × 20 mm and they were 3 mm thick. The sample was embedded in a square frame of adjustable size and pressed against the glass surface that was fixed on the lower board. The glass surface was wetted with distilled water and was driven to move horizontally and repeatedly in a velocity range of  $5 \times 10^{-4}$ – $3 \times 10^{-2}$  ms<sup>-1</sup> over a distance of 100 mm. Prior to the measurement, the glass plate was carefully washed with a cleaner, rinsed in distilled water, and dried in air. The measurements under various loads at a certain velocity were carried out using one sample, starting from the lower load and increasing the load continuously. The sliding-velocity dependence under a constant load was also measured in the same way. The detailed procedures are described elsewhere [10]. The frictional force per unit area (shear stress),  $f$ , and normal pressure,  $P$ , were calculated by dividing the frictional force,  $F$ , and load,  $W$ , by the surface area of the sample in the load-free state, respectively. The frictional coefficient,  $\mu$ , was calculated using the equation  $\mu = F/W$ .

Received: May 13, 2004

Final version: November 2, 2004

Published online: January 24, 2005

- [1] B. N. J. Presson, *Sliding Friction: Physical Principles and Applications*, 2nd ed., NanoScience and Technology Series, Springer, Berlin **1998**.
- [2] J. P. Gong, T. Kurokawa, T. Narita, G. Kagata, Y. Osada, G. Nishimura, M. Kinjo, *J. Am. Chem. Soc.* **2000**, *123*, 5582.
- [3] J. P. Gong, Y. Katsuyama, T. Kurokawa, Y. Osada, *Adv. Mater.* **2003**, *15*, 1155.
- [4] Y. Na, T. Kurokawa, Y. Katsuyama, H. Tsukeshiba, J. P. Gong, Y. Osada, S. Okabe, T. Karino, M. Shibayama, *Macromolecules* **2004**, *37*, 5370.
- [5] G. Kagata, J. P. Gong, Y. Osada, *J. Phys. Chem. B* **2002**, *106*, 4596.
- [6] H. Wang, G. A. Ateshian, *J. Biomech.* **1997**, *30*, 771.
- [7] C. W. McCutchen, *Lubrication of Joints, The Joints and Synovial Fluid*, Vol. 10, Academic, New York **1978**, p. 437.
- [8] T. Sadada, Y. Tsukamoto, K. Mabuchi, *Biotribology*, Sangyo-Tosyo, Tokyo, Japan **1988**.
- [9] J. P. Gong, G. Kagata, Y. Osada, *J. Phys. Chem. B* **1999**, *103*, 6007.
- [10] J. P. Gong, M. Higa, Y. Iwasaki, Y. Katsuyama, Y. Osada, *J. Phys. Chem. B* **1997**, *101*, 5487.

## Hydrogen Physisorption in Metal–Organic Porous Crystals\*\*

By Barbara Panella and Michael Hirscher\*

The major bottleneck for the commercialization of fuel-cell vehicles is onboard hydrogen storage.<sup>[1]</sup> The presently available systems are high-pressure tanks or liquefied hydrogen in

cryogenic vessels, which both possess severe disadvantages, e.g., large size and low consumer acceptance concerning safety aspects. The storage of hydrogen in light-weight solids could be the solution to this problem.<sup>[2]</sup> Hydrogen may be stored in solids by two principle mechanisms: i) Hydrogen atoms may be dissolved or form chemical bonds, i.e., chemisorption. ii) The adsorption of hydrogen molecules onto surfaces, i.e., physisorption. Chemisorption, or storage in metal hydrides, has the drawback of either low-storage capacity or high-release temperature. For physisorption, new nanoscale materials with high specific surface area are needed. During the past six years this area has been dominated by announcements of high-storage capacities in carbon nanostructures. However, a critical review shows that, around room temperature, carbon nanostructures cannot store the amount of hydrogen required for automotive applications.<sup>[3]</sup> Recently, a new class of crystalline material, which possesses a very low density and high surface area, the so-called metal–organic frameworks (MOFs) and similar porous materials, have been developed and synthesized.<sup>[4–8]</sup> A whole family of MOFs have been produced by linking Zn<sub>4</sub>O clusters with a variety of rigid organic linkers. For example, MOF-5,<sup>[5]</sup> wherein benzenedicarboxylate groups are used to form a three-dimensional cubic crystal. New hopes arose when hydrogen-storage capacities of 4.5 wt.-% at 77 K, and 1 wt.-% at room temperature, and a pressure of 20 bar were announced for these MOFs by Rosi et al.<sup>[9]</sup>

In this communication, we report detailed hydrogen-storage measurements for MOF-5, covering a larger range of applied hydrogen pressure.

The synthesis of a crystalline metal–organic framework from Zn<sub>x</sub>O subunits and benzenedicarboxylate as an organic linker was performed following the procedure of Huang et al.<sup>[10]</sup> zinc nitrate and the protonated form of benzenedicarboxylic acid (BDC) were dissolved in *N,N*-dimethylformamide (DMF), and triethylamine (TEA) was slowly added to the solution. Immediately after adding the organic base, a white product appeared in the solution. The same synthesis was repeated adding 3 drops of H<sub>2</sub>O<sub>2</sub> to the solution of zinc nitrate and BDC. In both cases, the X-ray diffraction pattern of the white solid were congruent with a Le Bail profile matching,<sup>[11]</sup> based on the crystallographic data of Li et al.,<sup>[6]</sup> showing that the product had space group *Fm-3m* like MOF-5, with a refined lattice parameter of 25.80 Å (Fig. 1).

The crystalline structure did not change after heating the sample under vacuum up to 200 °C, giving proof of its thermal stability. In contrast, after exposing the sample in air for six weeks we obtained a different X-ray diffraction pattern, indicating that the samples tend to decompose, as was also observed by Huang et al.<sup>[10]</sup> Both MOF-5 samples (synthesized with and without addition of H<sub>2</sub>O<sub>2</sub>) had a Brunauer–Emmett–Teller (BET) specific surface area (SSA) of 572 m<sup>2</sup> g<sup>-1</sup> and a Langmuir SSA of 1014 m<sup>2</sup> g<sup>-1</sup>, far below the value of 2900 and of 3362 m<sup>2</sup> g<sup>-1</sup> reported by the group of Yaghi.<sup>[6,12]</sup> Applying the *t*-method, we measured the volume of the micropores to be 0.28 g cm<sup>-3</sup>. After decomposition of the sample kept in air,

[\*] Dr. M. Hirscher, B. Panella  
Max-Planck-Institut für Metallforschung  
Heisenbergstr.3, D-70569 Stuttgart (Germany)  
E-mail: hirscher@mf.mpg.de

[\*\*] The authors are very grateful to Ewald Bischoff for taking the SEM images of the MOF-5 samples, to Annette Fuchs for the N<sub>2</sub> sorption measurements, and to Robert Dinnebier for the XRD profile matching.